Journal of the European Ceramic Society 17 (1997) 1325–1334

PII: S0955-2219(96)00235-X
0955-2219/97/$17.00

Comparison of the Oxidation Behaviour of Two Dense Hot Isostatically Pressed Tantalum Carbide (TaC and Ta_2C) Materials

M. Desmaison-Brut, N. Alexandre and J. Desmaison

Laboratoire de Matériaux Céramiques et Traitements de Surface LMCTS,
URA CNRS 320 - Université de Limoges, 123 Avenue Albert Thomas, 87060 Limoges Cedex, France

(Received 23 July 1996; revised version received 7 November 1996; accepted 11 November 1996)

Abstract

Isothermal oxidation of dense HIPed tantalum carbide materials TaC and Ta_2C, has been performed in flowing oxygen between 750 and 850°C.

The behaviour of the two carbides: i.e. TaC (NaCl type structure) and Ta_2C (hexagonal type), is characterized by the growth of a non-protective oxide scale which, on square section samples, forms a maltese cross. X-Ray diffraction analysis has only shown the formation of tantalum hemipentoxide βTa_2O_5. The oxidation of TaC proceeds by an interfacial reaction process. For Ta_2C, the mechanism could be more complex due to the presence of an intermediate oxycarbide layer TaC_xO_y which has been detected at the Ta_2C–Ta_2O_5 interface. Indeed, in this case, it is not possible to exclude a diffusion limiting process through this oxynitride sublayer of constant thickness with time. © 1997 Elsevier Science Limited.

Le comportement à l'oxydation dans l'oxygène de deux carbures de tantale denses TaC et Ta_2C a été étudié entre 750 et 850°C.

Dans les deux cas, la couche d'hémipentoxyde de tantale βTa_2O_5 s'ouvre progressivement au niveau des arêtes, sous l'effet des contraintes de croissance, en formant une croix de malte. Il en résulte que l'oxyde n'est pas protecteur. Concernant TaC, le mécanisme proposé fait intervenir un régime de réaction à l'interface carbure-oxyde. Dans le cas de Ta_2C, le mécanisme est certainement plus complexe, ceci en relation avec la formation d'une couche intermédiaire d'oxycarbure TaC_xO_y située à l'interface Ta_2C–Ta_2O_5. Dans ce cas, il n'est pas possible d'exclure un processus diffusionnel limitant à travers cette sous-couche d'oxynitrure d'épaisseur constante avec le temps.

1 Introduction

Transition metals such as tantalum, hafnium, zirconium, niobium, as well as their nitrides and carbides, are unstable in oxidizing atmospheres. Oxidation studies have been carried out on powders, wires or platelets, but, for dense sintered materials, there is still a considerable lack of kinetic data. In the past, attention has concentrated on the transition metal carbides[1–3] with few works being concerned with the sintering of tantalum carbide TaC.[4–6]

Tantalum monocarbide TaC (NaCl type structure) constitutes the matrices of hard alloys for the machining of materials. In the large homogeneity range for the fcc phase of the TaC system, evaluation of such properties as microhardness, electrical resistivity or superconductivity[7,8] exists.

The phase diagram of the tantalum–carbon system shows another well-defined carbide, Ta_2C. This hemicarbide Ta_2C has a structure based on a hexagonal closest-packed metal lattice with the carbon atoms filling one half of the octahedral holes.[9,10]

So far, very few papers appear to have been published on the oxidation behaviour of tantalum carbide TaC and none on the hemicarbide Ta_2C. The oxidation of hot-pressed TaC has been studied between 1700 and 2200°C, for an oxygen partial pressure varying from 10^{-3} to 10^{-1} Pa.[11] No oxide layer was formed, but the authors observed a carbon diffusion from the heart to the surface which was considered as the limiting step. They concluded, on the basis of the few results obtained, that the oxidation behaviour of TaC and NbC was qualitatively the same.

Consequently, in view of this great lack of data, it was of interest to investigate the difference in reactivity of the two tantalum carbides.

2 Experimental Procedure

The tantalum carbide powder, TaC, was supplied by H. C. Starck and the commercially available powder, Ta_2C, by Cerac. The main characteristics of the starting powders are presented in Table 1. The same HIP treatment has been applied on the two initial powders. After being cold isostatically pressed at 200 MPa, the green compact was introduced inside a titanium container. A carbon layer was necessary to prevent any chemical reaction between the capsule and the component. After degassing in vacuum at 600°C for 10 h, the container was sealed and HIPed at 1630°C, under 195 MPa pressure. The dwell time lasted 2 h.

The relative densities of the specimens treated by HIP, were greater than 98%. Calculations done on the dense TaC material and based on the lattice parameter value (0·4454 nm) indicated that the fcc carbide is slightly unstoichiometric ($TaC_{0.99}$).

The oxidation resistance was tested in a dynamic flow of pure oxygen ($5{\cdot}6 \times 10^{-3}$ litre/s), at atmospheric pressure, using a Setaram microbalance. Cubic samples (4 mm side) were polished, washed in alcohol with ultrasonic assistance and dried. The procedure was as follows: first, the furnace was evacuated (10^4 Pa) and a stream of argon was introduced. As the temperature was increased, the specimen was kept out of the hot zone until 15 min after the introduction of oxygen when it was lowered with a magnetic device into the hot zone. The zero time was taken when the platinum crucible containing the sample reached the hot zone.

The kinetic curves were obtained by plotting the fractional weight change α ($\alpha = \Delta m/\Delta m_\infty$) versus time. The weight gain Δm_∞ corresponds to the complete oxidation evaluated by considering that TaC or Ta_2C is transformed into Ta_2O_5 according to the reactions:

$$2\ TaC + 9/2\ O_2 \rightarrow Ta_2O_5 + 2\ CO_2 \qquad (1)$$

$$Ta_2C + 7/2\ O_2 \rightarrow Ta_2O_5 + CO_2 \qquad (2)$$

In order to have an idea of the reactivity of the materials, a sample of each type was exposed to oxygen with a linear increasing temperature of 17×10^{-3}°C/s. The nonisothermal oxidation curves of Fig. 1 show that the hemicarbide material is more oxidation resistant than the monocarbide.

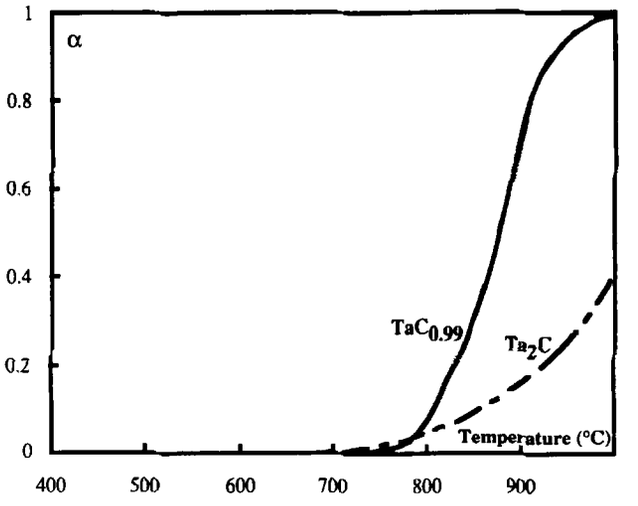

Fig. 1. Non-isothermal oxidation curves for cubic samples exposed to flowing oxygen at 1 atm.

3 Oxidation Behaviour of Tantalum Carbide, TaC

3.1 Effect of temperature

Isothermal curves have been recorded at atmospheric pressure, between 750 and 850°C (Fig. 2). Their shape is quasi-linear at low temperatures but shows some deceleration in the upper temperature range. After being kept 5 h at 850°C, the specimen is totally oxidized. A master run was chosen in the middle of the series and a factor A was calculated for any curve such that multiplication of the time scale of the run by A would superimpose onto the master run curve. Each curve can be superimposed onto any other by such an affinity relationship with time (Fig. 3). As log A is found to be a linear function of $1/T$, the activation energy value calculated ($E = 379 \pm 16$ kJ/mol) is unique over this range of temperature.

3.2 Effect of pressure

Isobaric curves have been recorded at 800°C, in the pressure range 0·2 to 1×10^5 Pa, and plotted as a function of time (Fig. 4). The general shape of the kinetics is retained and the curves can again be superimposed (Fig. 5).

3.3 Morphological observations

During the first minutes of the reaction, a grey oxide film is formed. As time and temperature increase, the sintering of the oxide scale, facilitated by the presence of the initial powder impurities,

Table 1. Powders characteristics and composition

Powders	d_{th}	*Lattice parameters*		*Mean diameter*	*Specific area*	*Elements (mass %)*		
		a (*nm*)	c (*nm*)	$\varnothing_{eq}$ (μm)	(m^2/g)	*C*	*O*	*Fe*
TaC	14·34	0·4454	—	2·0	1·16	6·29	0·26	0·004
Ta_2C	14·90	0·3103	0·4937	4·5	0·25	3·17	0·25	0·001

is performed. For a given temperature (800°C), the oxide scale thickness may be related to the reaction time by a linear law and the time dependence of the TaC (unreacted) core thickness is given in Fig. 6. X-ray analysis shows only the presence of the oxide βTa_2O_5 independently of pressure and temperature. Figures 7(a) and 7(b) show the columnar aspect of the tantalum oxide. The high value of the Pilling and Bedworth ratio (Δ = 2·13) induces stresses in the scale. The good adherence of the oxide to the core does not allow stress relaxation by spalling but leads to the opening of the cube edges and to the formation of a maltese cross (Fig. 7(b)). The same process has already been observed in the case of the oxidation behaviour of a dense and HIPed TaN material.[12] The oxide surface aspect is different at 825°C or lower than at 850°C (Figs 7(c) and (d)) certainly due to the better sintering of the external part.

3.4 Interpretation

The kinetic results indicate that the reaction rate V is a function of pressure and temperature. As both isothermal and isobaric curves are in a close affinity relationship with time, the equation can be written in a separated variables form:

$$V = \frac{d\alpha}{dt} = f(\alpha)g(T)h(P) = \text{Cte}\, f(\alpha)h(P)\exp -\frac{E}{RT} \quad (3)$$

where $f(\alpha)$ is a morphological term characteristic of the reaction area and Cte is a constant.

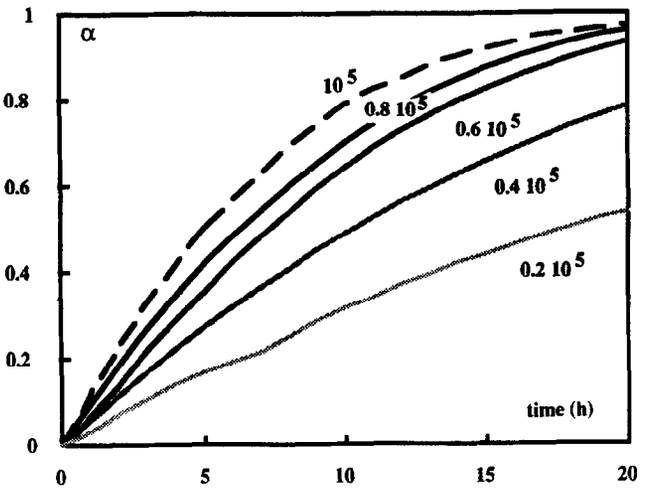

Fig. 4. Isobaric curves recorded at 800°C, in the pressure range 0·2 to 1 × 10^{55} Pa.

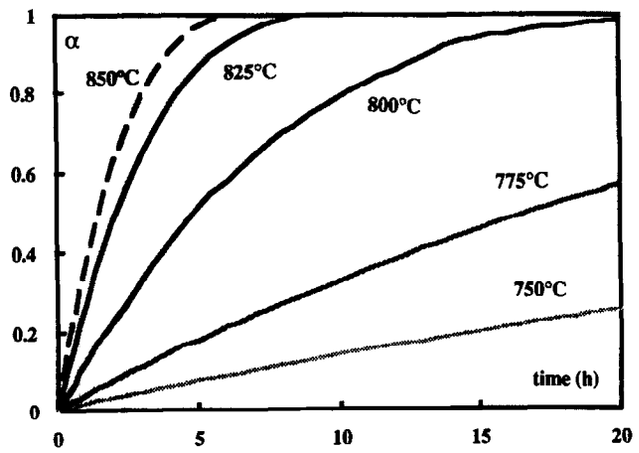

Fig. 2. Isothermal curves recorded at 1 atm in the temperature range 750–850°C.

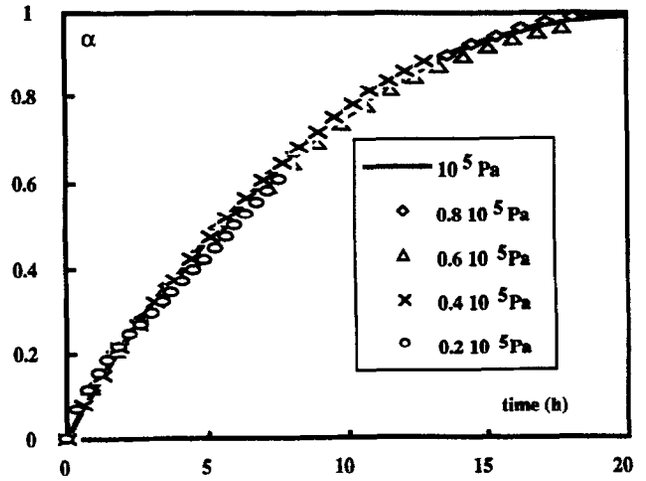

Fig. 5. Superimposed isobaric curves.

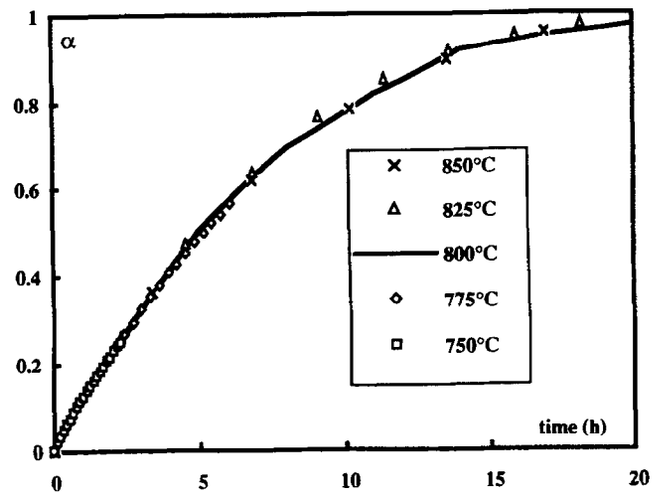

Fig. 3. Superimposed isothermal curves.

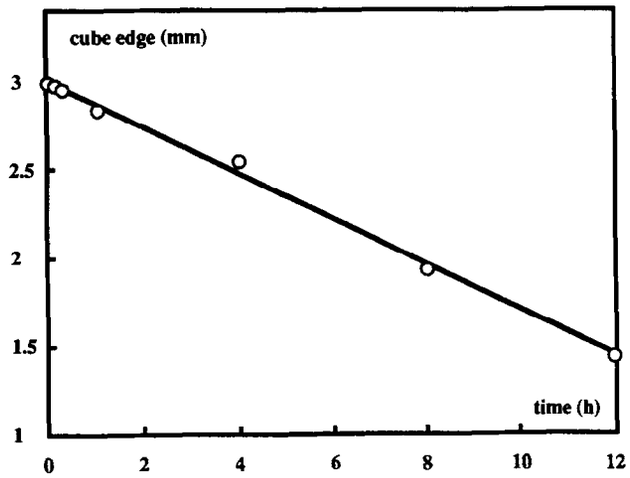

Fig. 6. Time dependence of tantalum carbide core thickness at 800°C.

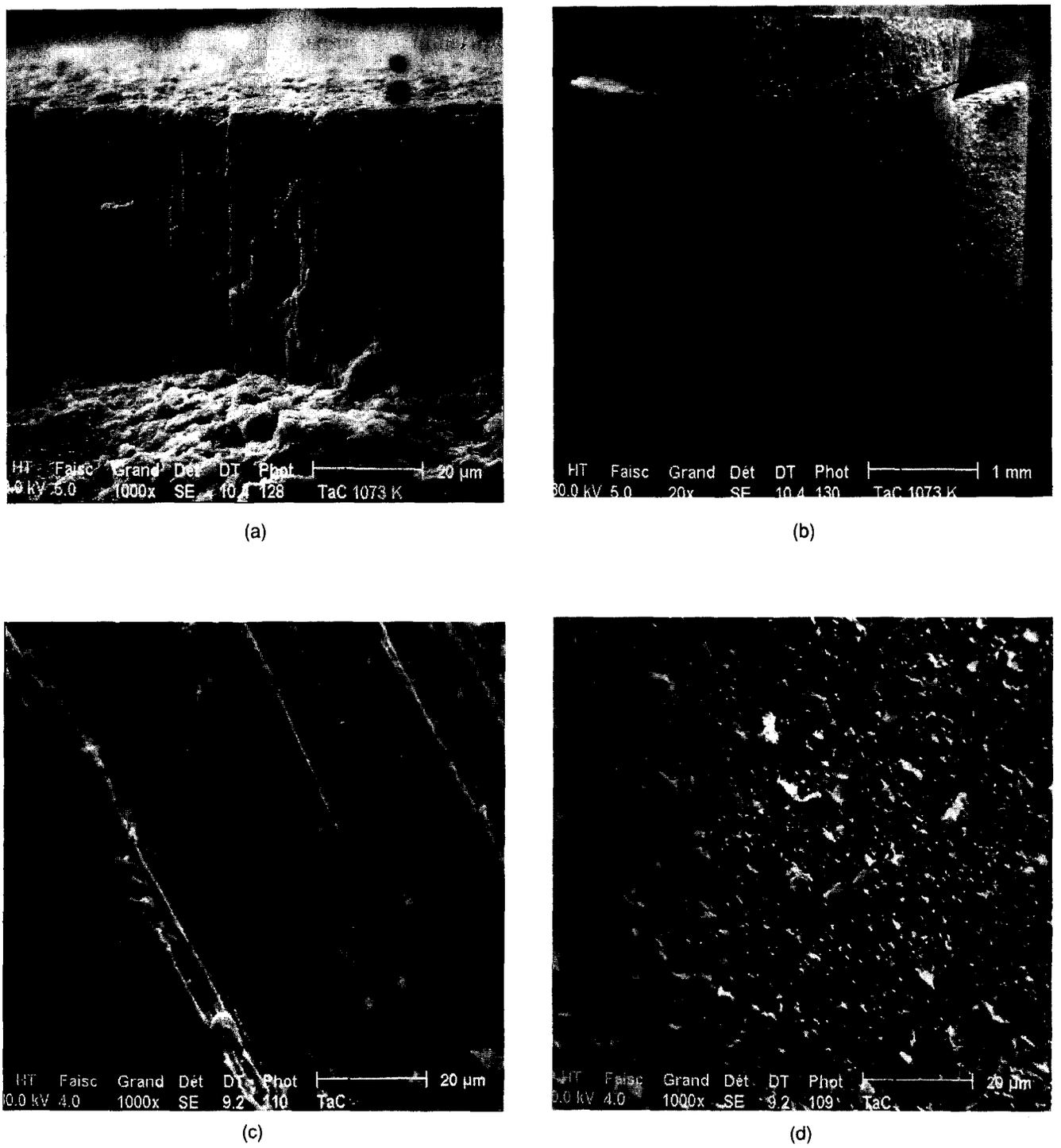

Fig. 7. SEM of oxidized TaC materials: (a) 800°C, 15 min, cross–section; (b) 800°C, 4 h, cross-section; (c) 825°C, 20 h, surface; (d) 850°C, 20 h, surface.

This means that the controlling process is unique and identical to itself over the whole reaction range.[12,13] At constant temperature and pressure, the shape of the curves is determined only by geometrical factors.

The oxide porosity and the opening of the cube edges at the beginning of the reaction allow direct access of oxygen at the carbide–oxide interface. On the other hand, the carbon dioxide gas release from the core is easy. All these remarks suggest a reaction regime at this inner interface. Therefore, the reaction rate V is directly proportional to the surface area of the non-oxidized cubic carbide core of edge a, at time t.

$$V = \frac{d\alpha}{dt} = K(T,P)S(\alpha) \qquad (4)$$

$S(\alpha) = 6\,a^2$ being related to the conversion degree α through a.

Indeed: $\alpha = 1 - v/v_0$

with v the volume of the residual substrate and v_0 the volume of the initial cube of edge a_0. By extension:

$$\alpha = 1 - \frac{a^3}{a_0^3} \tag{5}$$

$$a = a_0 (1 - \alpha)^{1/3} \tag{6}$$

The rate law becomes:

$$\frac{d\alpha}{dt} = 6\, K(T,P)\, a_0^2 (1 - \alpha)^{2/3} \tag{7}$$

Integration of expression (7) leads to:

$$F(\alpha) = 1 - (1 - \alpha)^{1/3} = kt \tag{8}$$

with $k = 2\, a_0^2\, K(T,P)$.

Therefore, the assessment of the validity of our kinetic model may be found by plotting $F(\alpha)$ versus t (Fig. 8). As can be seen, linear plots are obtained for all temperatures.

By plotting log k versus reciprocal temperature (Fig. 9), a value of 385 ± 11 kJ/mole is calculated. In the same way, at various pressures, a linear relation is obtained, for example at 800°C, by plotting $F(\alpha)$ versus time (Fig. 10).

The constant dependence with pressure may be represented by a relation of the form:

$$k = aP/(1 + bP) \tag{9}$$

where: $a = 0{\cdot}067$ and $b = 0{\cdot}781$ (Fig. 11)

The observed pressure dependence may be explained by assuming that an adsorption equilibrium of molecular oxygen preceeds the formation of Ta_2O_5:

$$O_2 + s \Leftrightarrow O_2 - s \tag{10}$$

According to the Langmuir model, the fraction θ_G of adsorption sites s occupied by chemisorbed oxygen is:

$$\theta_G = \frac{K_1 P_{O_2}}{1 + K_1 P_{O_2}} \tag{11}$$

where K_1 is the equilibrium constant of reaction (10).

If the oxidation rate is proportional to the number of adsorbed oxygen molecules,

$$v = k_0 \theta_G = \frac{K_2 P_{O_2}}{1 + K_1 P_{O_2}} \tag{12}$$

with $K_2 = k_0 K_1$

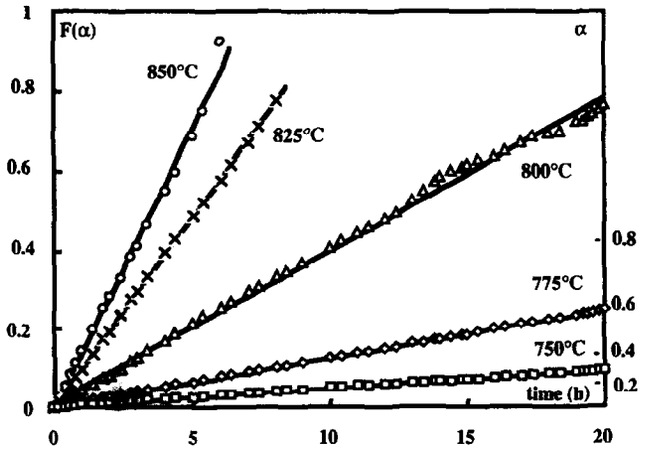

Fig. 8. Oxidation curves plotted against time in the cubic form, at various temperatures.

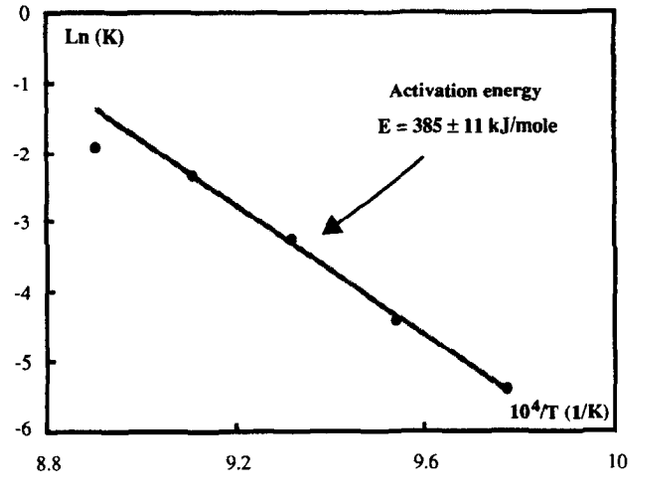

Fig. 9. Influence of temperature on the rate constant K at 1 atm.

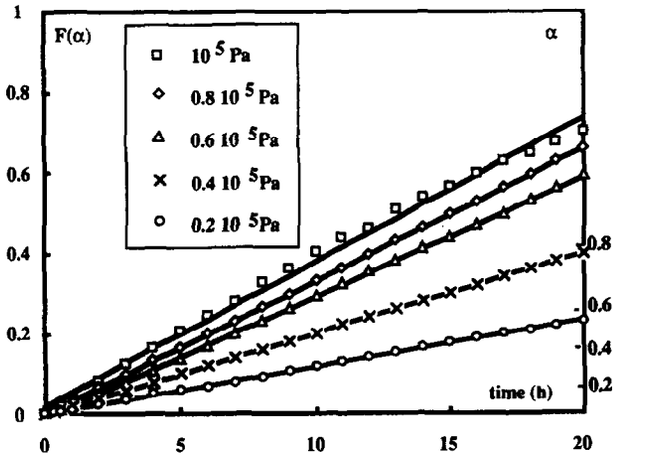

Fig. 10. Oxidation curves plotted against time in the cubic form, at various pressures (800°C).

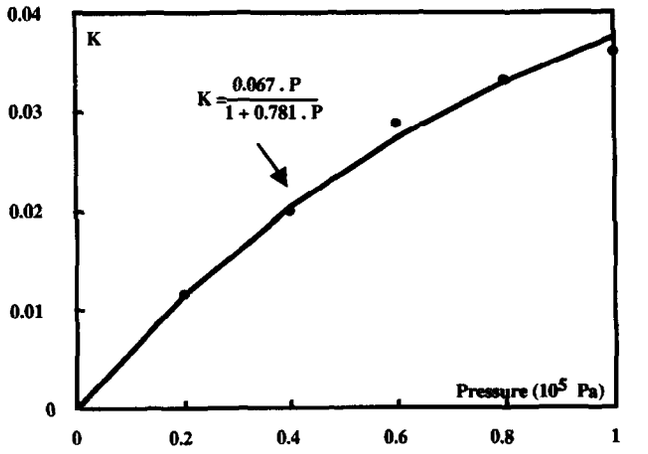

Fig. 11. Effect of oxygen pressure on the rate constant at 800°C.

Finally, a parametric kinetic law of type (3) may represent the oxidation rate:

$$V = \text{Cte}\,(1 - \alpha)^{2/3}\ 0{\cdot}067\ P/(1 + 0{\cdot}781\ P)$$
$$\exp(-385\,000/RT) \qquad (13)$$

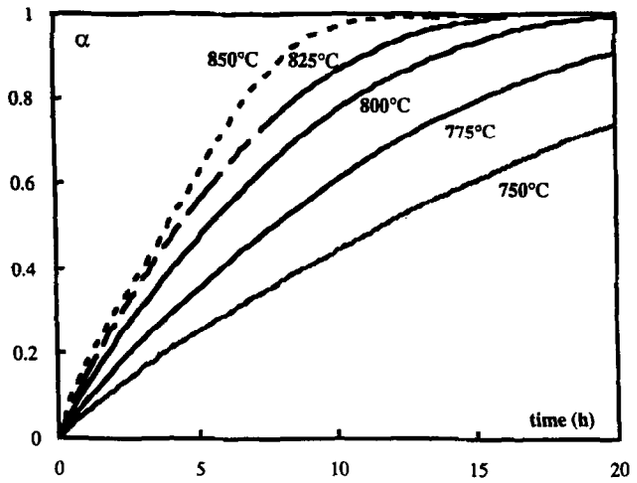

Fig. 12. Isothermal curves recorded at 1 atm in the temperature range 750–850°C.

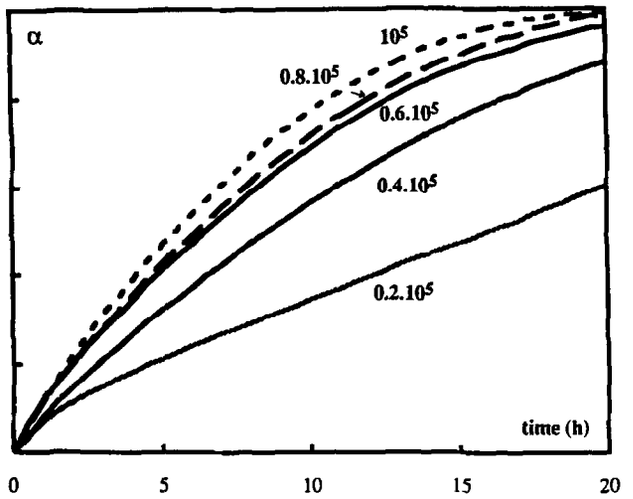

Fig. 13. Isobaric curves recorded at 800°C, in the pressure range 0·2 to 1 × 10^5 Pa.

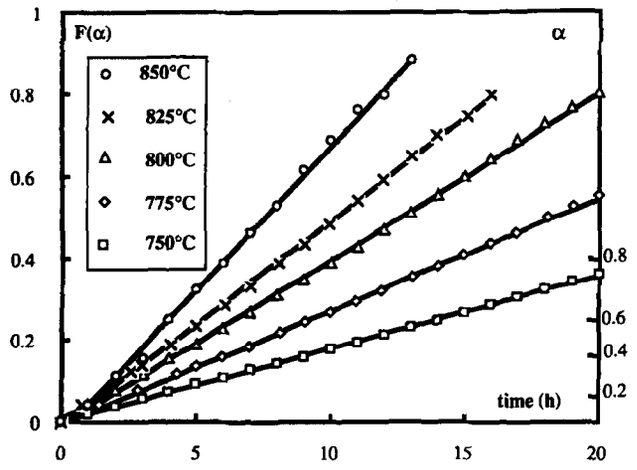

Fig. 14. Oxidation curves plotted against time in the cubic form, at various temperatures.

4 Oxidation Behaviour of Tantalum Hemicarbide Ta_2C

4.1 Effect of temperature and pressure

An identical study has been performed on the tantalum hemicarbide ceramic. The results have been

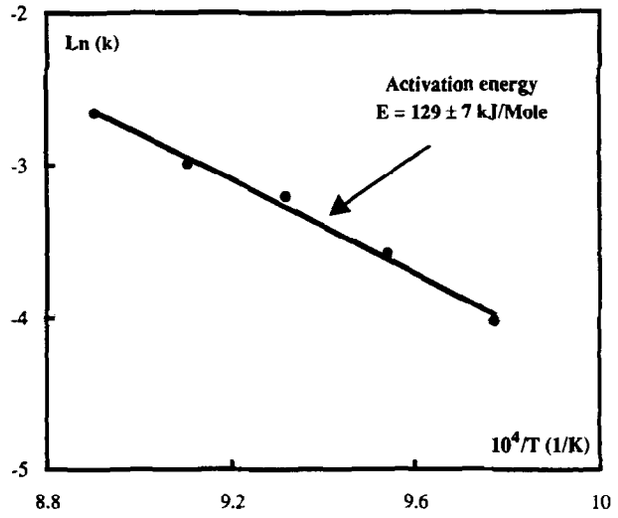

Fig. 15. Influence of temperature on the rate constant K at 1 atm.

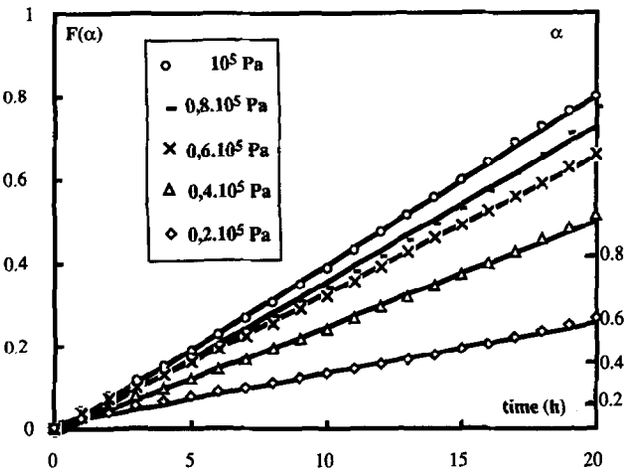

Fig. 16. Oxidation curves plotted against time in the cubic form, at various pressures.

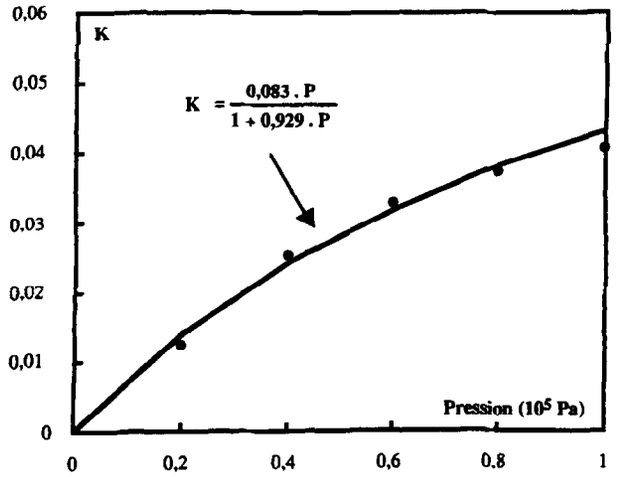

Fig. 17. Effect of oxygen pressure on the rate constant at 800°C.

analysed by the same mathematical approach and appear in Figs 12–17.

The global kinetic law may be written in the form:

$$V = \mathrm{Cte}(1 - \alpha)^{2/3}\ 0{\cdot}083\ P/(1 + 0{\cdot}929\ P)$$
$$\exp(-129\,000/RT) \qquad (14)$$

4.2 Morphological observations

X-ray analysis shows the presence of β Ta_2O_5 independently of pressure and temperature. The hemipentoxide which forms a maltese cross is rather dense and adherent to the core (Figs 18(a) and (b)). By optical microscopy, we have observed that the oxidation starts at the grain boundaries of the Ta_2C ceramic. On cross-sections, a layer with a maximum thickness of 20–25 μm is present at the interface Ta_2O_5–Ta_2C (Fig. 18(c)). The maximum thickness seems to be independent of time but the layer disappears near the edges of the cube. The microhardness value of the Ta_2O_5 phase is low (H_V^{5N} 3·5 ± 0·5 GPa) compared to the microhardnesses of the intermediate phase

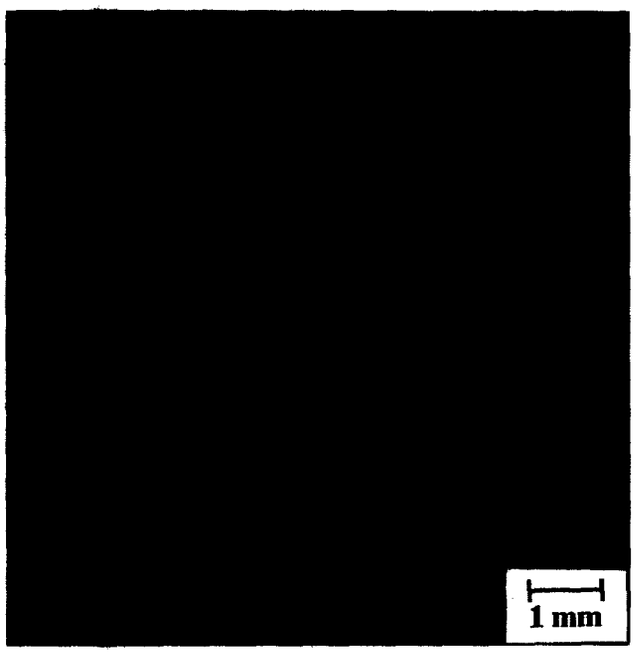

(a)

(b)

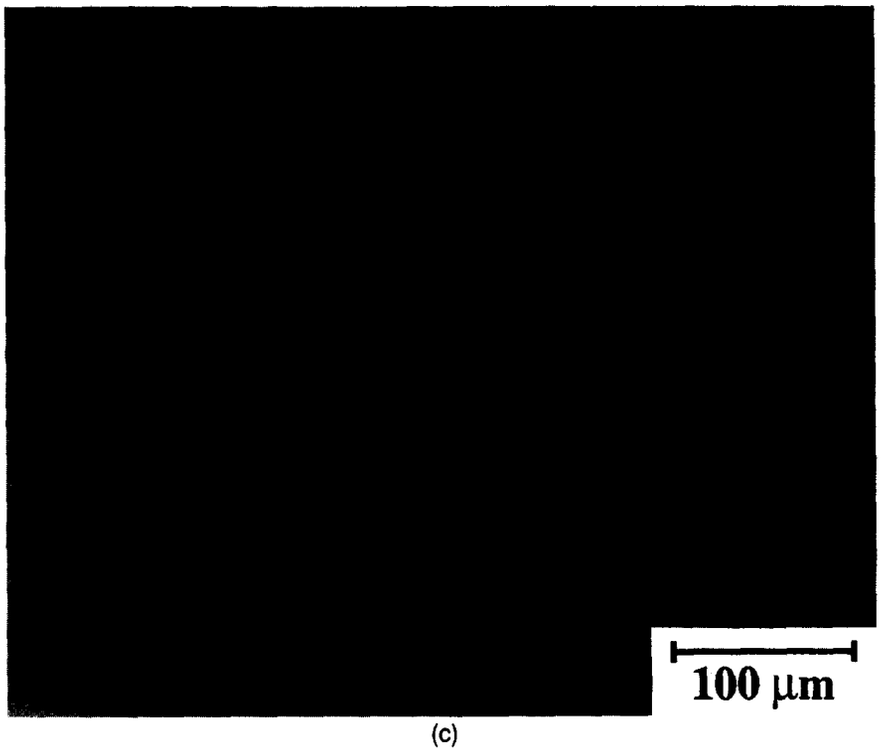

(c)

Fig. 18. Micrographs of oxidized Ta_2C materials: (a) 750°C, 20 h (optical micrograph); (b) 750°C, 20 h (scanning electron micrograph); (c) 800°C, 20 h (optical micrograph).

(12·1 ± 0·9 GPa) and of the tantalum hemicarbide Ta_2C (10·7 ± 0·9 GPa).

By X-ray analysis of successively polished surfaces through the intermediate layer, we have noticed an evolution of the lattice parameters of the Ta_2C grade.

The EDAX analysis of the carbon, oxygen and tantalum elements and their EPMA profiles clearly show the presence, through the interface, of both carbon and oxygen[14] suggesting the formation of a tantalum carboxide layer.

5 Oxidation in These and Other Carbide Systems

5.1 Comparison of the oxidation behaviour of the two carbides TaC and Ta_2C

In our case, the correlation of morphological observations with kinetic results is readily made. In both cases, the densification of tantalum pentoxide was not sufficient to lead to a restricted access of oxygen to the TaC surface; as a consequence, there was no requirement for the existence of a diffusion-limiting step.

In addition, due to the sample geometry, a maltese cross is formed. However, the Ta_2C core does not keep as perfect a cubic shape as it does in the case of the oxidation of tantalum carbide TaC (Figs 7 and 18(a)). Raman spectra in the latter case have not suggested the presence of free carbon within the scale. Therefore, for TaC, the liberated carbon may react directly with oxygen to form CO_2. The columnar oxide scale allows an easy outward diffusion of this gas.

In both cases, the reactions appear to be governed by an interfacial process[21–23] located at the carbide–oxide interface. However, the hemicarbide exhibits a higher oxidation resistance perhaps due to the transitory formation of the oxycarbide phase.

The monocarbide TaC has a fcc structure where the carbon atoms are located inside the octahedral sites. When the material is unstoichiometric, the vacant sites can be occupied by oxygen atoms but here a limited number of such sites are available as the monocarbide is almost stoichiometric ($TaC_{0.99}$). The presence of an oxycarbide layer has not been detected even after a few minutes of oxidation treatment.

On the other hand, the hexagonal anti-CdI_2 type crystal structure of Ta_2C where the carbon atoms are occupying only one plane out of two, could facilitate the dissolution of oxygen and the insertion of oxygen atoms inside the Ta_2C network with the formation of a tantalum carboxide layer preceding the growth of the hemipentoxide scale.

The observation of cross-sections shows that this reaction starts preferentially at the grain boundaries of the substrate and proceeds at an almost constant speed. Therefore, in this case, we cannot exclude a diffusion limiting step through an oxynitride sublayer of constant thickness with time.

5.2 Comparison with other published works on oxidation of carbide materials

The formation of such interlayers has been reported in other studies devoted to the oxidation of several transition carbides (HfC[15–18], ZrC[19–23], TiC[24], NbC[25]).

After hafnium carbide CVD films have been oxidized at temperatures in the range of 1400 to 2060°C, three distinct layers are observed: (a) a residual hafnium carbide layer, (b) a dense-appearing hafnium oxide interlayer containing carbon, and (c) a porous outer layer of hafnium oxide.[15] As the overall duplex oxidized layer appeared to be protective, Bergeron *et al.*[15] solved the diffusional problem by combining experimental measurements of layer thicknesses and oxygen concentrations with an extended formulation of the moving-boundary diffusion theory. The results indicate that the oxide interlayer is a better diffusion barrier for oxygen than either of the other layers.

In the case of not fully densified sintered materials, the formation of a less prominent dark black interlayer has also been described.[16] However, the carbide could first dissolve oxygen, up to 30% at 2000°C,[17] before it converts to a compact oxygen-deficient oxide. The transformation occurs prior to full oxidation of the carbide when there is insufficient oxygen to oxidize all the carbon to CO. The integrity and low porosity of the interlayer indicate that potential gas production is not effective in creating a disruption at interfaces or separation between layers.[15]

The isothermal oxidation of HfC powders, at relatively low temperatures (480–600°C), proceeds by similar processes.[18] After an initial rapid oxidation with the formation of oxycarbide, HfC_xO_{1-y}, oxidation proceeds by a diffusion-controlled process in the early stage (10–50% oxidation) followed by a phase-boundary-controlled process in the later stage (>50%). The change in oxidation mechanism is associated with the generation of cracks on the grains, resulting from the growth or expansion stress due to the formation of monoclinic HfO_2. The formation of amorphous carbon in the oxidized samples was suggested by Raman spectra, this carbon being difficult to remove at low oxygen pressures and temperatures.

Carbon-containing oxide scales have also been obtained by oxidation of powders,[19,20] sintered

materials[21,22] or single crystals[23] of zirconium carbide. Dufour *et al.*[19] and Shimada *et al.*[20] have suggested the formation of carbon during oxidation of ZrC powders. No satisfactory explanation for the oxidation of ZrC powders has been given in view of the varied kinetic results, and with regard to the influence of cracking on oxidation. Barnier *et al.*[21,22] also assumed that a certain amount of carbon is retained in the oxycarbide structure. They have reported that the oxidation kinetics of sintered ZrC, in the temperature range of 400 to 700°C, under 130 kPa of oxygen, are successively controlled by a diffusion process and by a phase-boundary process.

More recently, Shimada *et al.*[20] carried out the isothermal oxidation of ZrC single crystals with (100) orientation at temperatures of 500°, 550° and 600°C at an oxygen pressure of 2·6 kPa for times up to 240 h. It was found that the oxide scale was divided into two regions, zones 1 and 2, which contained 14–23 and 7–10 at% carbon, respectively. The thickness of zone 1, consisting of a compact, pore-free matrix of cubic ZrO_2, increased parabolically up to 240 h at 500°C and probably in an early period at 550 and 600°C, reaching a constant thickness of about 2–3 μm. In contrast, the thickness of zone 2, where some growth and aggregation of the c-ZrO_2 occurred, producing 5- to 20-nm sized particles, increased linearly with time.

The oxidation mechanism of titanium carbide powders at low temperatures (350–500°C) has not yet been clearly elucidated. Shimada *et al.*[24] reported the formation of oxycarbide/titanium suboxides and the crystallization of anatase, followed by the generation of cracks in the grains.

The oxidation behaviour of powder and single crystals of niobium carbide is also complex. However, recent kinetic results[25] suggested that the oxidation of both samples proceeds essentially by a phase-boundary-controlled reaction due to the formation of columnar, porous Nb_2O_5 grains, with the major axis normal to the surface facilitating CO_2 evolution.

6 Model for the Oxidation Mechanism of Ta_2C

None of the preceding approaches is adequate to explain the present results. On the contrary, the paralinear oxidation model,[26] first discussed by Loriers[27] in an interpretation of the oxidation of cerium (growth of porous CeO_2 on compact Ce_2O_3) could be of particular interest. Indeed, this model, used by other authors, for instance for the oxidation of tungsten[28] and calcium,[29] describes the growth of multilayered scales where an inner compact oxide grows at a parabolic rate and is simultaneously oxidized to a higher oxide with no protective properties.

In the case of plane symmetry, the growth of the two layers may be described by the equations:[26,29]

$$dy/dt = a/y - b \tag{15}$$

$$dz/dt = b \tag{16}$$

where y and z represent the mass gain per unit area in the compact layer and in the porous layer; a and b are constants.

The integration of these equations gives the growth law of each scale:

$$y = a/b \log (1 - b/ay)^{-1} - bt \tag{17}$$

$$z = bt \tag{18}$$

and the total oxidation rate of the paralinear oxidation in terms of mass gain x:

$$x = y + z = a/b \log [1 - b/a (x - bt)]^{-1} \tag{19}$$

During initial oxidation, the parabolic growth predominates and corresponds to the growth of y. When $a/y = b$ the growth rate of the compact layer is equal to zero and y reaches a maximum value:

$$y_{max} = a/b \tag{20}$$

Then the reaction proceeds at constant rate:

$$dx/dt = a/y_{max} = b \tag{21}$$

corresponding to linear kinetics.

When this pseudo-linear regime is established, the flow rate of diffusing species may be derived[30] from the well-known Fick's first law:

$$\frac{d\alpha}{dt} = DS \frac{\Delta C}{y_{max}} = K_D S \tag{22}$$

where D, S and ΔC are respectively the diffusion coefficient, the reactive area, the oxygen concentration variation and K_D a rate constant. Therefore, this equation being identical to (4) explains why linear $F(\alpha) = kt$ plots have been observed. Incidentally, the pressure dependence may be explained in the same way as the preceding case (TaC). The only problem with this approach is that we were not able to detect the initial period corresponding to the formation of the oxycarbide layer.

7 Conclusion

The aim of this work was to compare the oxidation behaviour of two hot isostatically pressed tantalum carbide materials TaC and Ta_2C.

The investigations have been done in dry oxygen, at the atmospheric pressure or lower.

Among the two materials, tantalum hemicarbide Ta_2C possesses the higher oxidation resistance. Different microstructures of the hemipentoxide Ta_2O_5 are formed and different activation energies are calculated (129 and 385 kJ/mol.) depending on the carbide (Ta_2C, TaC). An interfacial limiting process is shown to be developed during the 20 hours oxidation of the TaC grade.

Concerning Ta_2C, the mechanism is certainly more complex. The presence of an oxycarbide layer TaC_xO_y has been observed at the Ta_2C–Ta_2O_5 interface and may be explained by the hexagonal Ta_2C structure which presents empty layers of carbon atoms. These vacancies may be occupied by the oxygen atoms and a steady-state layer thickness is formed independently of time. Consequently, it is not possible to exclude a diffusion limiting step through the oxynitride layer. This change in mechanism could explain the difference in reactivity and activation energy observed for these two carbides.

References

1. Storms, E. K., *The Refractory Carbides, Refractory Materials*, Vol. 2. Academic Press, New York and London, 1967.
2. Toth, L. E., *Transition metal carbides and nitrides, chemical engineering, materials sciences.* Academic Press, New York and London, 1971.
3. Santoro, G., Variation of some properties of tantalum carbide with carbon content. *Trans AIME*, 1963, **227**, 1361–1368.
4. Kislyi, P. S., Shvab, S. A. and Egorov F. F., Sintering kinetics of tantalum carbide. *Porosh. Metall.*, 1982, **10**, 16–19.
5. Sautereau, J. and Mocellin, A., Sintering behaviour of ultrafine NbC and TaC powders. *J. Mat. Sci.*, 1974, **9**, 761–771.
6. Leipold, M. H. and Becher, P. F., Pressure densification in tantalum carbide. *Am. Ceram. Soc. Bull.*, 1970, **49**, 647–651.
7. Samsonov, G. V. and Rukina, V. B., Microhardness and electrical resistance of tantalum carbide in their homogeneous region. *Dopovidi Akad. Nauk Urk. RSR*, 1957, **3**, 247–249.
8. Giorgi, A. L., Effect of composition of the superconducting transition temperature of tantalum carbide and niobium carbide. *Phys Rev.*, 1962, **125**, 837–838.
9. Bowman, A. L., Wallace, T. C., Yarnell, J. L., Wenzel, R. G. and Storms, E. K., The crystal structures of V_2C and Ta_2C. *Acta Cryst.*, 1965, **19**, 6–9.
10. Hiraga, K. and Hirabayashi, M., Long range and short range order in interstitial compounds M_2X with special reference to V_2C and Nb_2C. *Journal de Physique*, 1977, **38**, C7-224–226.
11. Szokefalvi-Nagy, A. and Jehn, H., High-temperature oxidation of niobium carbide and tantalum carbide at low oxygen pressures. *Z. Metallkd.*, 1984, **75**, 389–394.
12. Montintin, J. and Desmaison-Brut, M., Oxidation behaviour of hot-isostatic-pressed tantalum nitride. In *High Temperature Corrosion of Technical Ceramics*, ed. R. J. Fordham. Elsevier Applied Science, London and New York, 1989, pp. 121–130.
13. Lefort, P., Ado, G. and Billy, M., Mécanisme de l'oxydation de l'oxynitrure d'aluminium fritté. *Rev. Int. Hautes Tempér. Réfract.*, 1990, **26**, 153–162.
14. Desmaison-Brut, M., Alexandre, N., Desmaison, J., Valin, F., Boncoeur, M. and Gogotsi, Y., Formation of an oxycarbide at the interface Ta_2C/Ta_2O_5 during the oxidation of a HIPed Ta_2C ceramic. *J. Solid Stat. Ionics*, in press.
15. Bargeron, C. B., Benson, R. C., Jette, A. N. and Phillips, T. E., Oxidation of hafnium carbide in the temperature range 1400° to 2060°C. *J. Am. Ceram. Soc.*, 1993, **76**, 1040–1046.
16. Holcomb, G. R., The high temperature oxidation of hafnium carbide. Ph.D. Dissertation, Ohio State University, Columbus, OH, USA, 1988.
17. Constant, K., Kieffer, R. and Ettmayer, P., On the pseudo-ternary system HfO–HfN–HfC. *Monatsh. Chem.*, 1975, **106**, 973–981.
18. Shimada, S., Inagki, M. and Matsui, K., Oxidation kinetics of hafnium carbide in the temperature range of 480 to 600°C. *J. Am. Ceram. Soc.*, 1992, **75**, 2671–2678.
19. Dufour, L. C. and Simon, J., Cinétique d'oxydation sous faible pression d'oxygène d'échantillons pulvérulents de monocarbures de zirconium et de tungstène et d'hémicarbure de molybdène. *Bull. Soc. Chim. Fr.*, 1968, **9**, 3643–3651.
20. Shimada, S. and Ishii, T., Oxidation kinetics of zirconium carbide at relatively low temperatures. *J. Am. Ceram. Soc.*, 1990, **73**, 2804–2808.
21. Barnier, P. and Thévenot, F., A comparative study of the oxidation resistance of zirconium carbide and zirconium oxycarbide, *Eur. J. Solid State Inorg. Chem.*, 1988, **25**, 495–508.
22. Barnier, P. and Thévenot, F., Synthesis and hot-pressing of single phase ZrC_xO_y and two phase ZrC_xO_y–ZrO_2 materials. *Int. J. High Technol. Ceram.*, 1986, **2**, 291–307.
23. Shimada, S., Nishisako, M. and Inagaki, M., Formation and microstructure of carbon-containing oxide scales by oxidation of single crystals of zirconium carbide. *J. Am. Ceram. Soc.*, 1995, **78**, 41–48.
24. Shimada, S. and Kozeki, M., Oxidation of TiC at low temperatures. *J. Mat. Sci.*, 1992, **27**, 1869–1875.
25. Shimada, S., A kinetic and thermoanalytical study on oxidation of powder and single-crystal samples for niobium carbide. *Oxidation of Metals*, 1994, **42**, 357–373.
26. Kofstad, P., *High Temperature Corrosion.* Elsevier Science Publishers, London, 1988.
27. Loriers, J., Loi d'oxydation du cérium métallique. Généralisation à d'autres métaux. *Compt. Rend. Acad. Sci. Paris*, 1950, **231**, 522–524.
28. Webb, W. W., Norton, J. T., and Wagner, C, Oxidation of tungsten. *J. Electrochem. Soc.*, 1956, **103**, 107–111.
29. Streiff, R., Etude de l'oxydation du calcium massif. Mécanismes de la réaction. *Acta Met.*, 1968, **16**, 1227–1238.
30. Billy, M. and Valensi, G., Reaction velocity of metalloids with metals, when the interfacial reactions are accompanied by diffusion: application to sulfur–silver reaction. *J. Chim. Phys.*, 1956, **53**, 832–844.